SANDIA REPORT
SAND2007-
Unlimited Release
Printed September 2007

Reliability of Materials in MEMS: Residual Stress and Adhesion in a Micro Power Generation System

M. S. Kennedy, D. F. Bahr, N. R. Moody

Prepared by
Sandia National Laboratories
Albuquerque, New Mexico 87185 and Livermore, California 94550

Sandia is a multiprogram laboratory operated by Sandia Corporation,
a Lockheed Martin Company, for the United States Department of Energy's
National Nuclear Security Administration under Contract DE-AC04-94AL85000.

Issued by Sandia National Laboratories, operated for the United States Department of Energy by Sandia Corporation.

Available to DOE and DOE contractors from
U.S. Department of Energy
Office of Scientific and Technical Information
P.O. Box 62
Oak Ridge, TN 37831

Telephone: (865) 576-8401
Facsimile: (865) 576-5728
E-Mail: reports@adonis.osti.gov
Online ordering: http://www.osti.gov/bridge

Available to the public from
U.S. Department of Commerce
National Technical Information Service
5285 Port Royal Rd.
Springfield, VA 22161

Telephone: (800) 553-6847
Facsimile: (703) 605-6900
E-Mail: orders@ntis.fedworld.gov
Online order: http://www.ntis.gov/help/ordermethods.asp?loc=7-4-0#online

SAND2007-6070
Unlimited Release
Printed September 2007

Reliability of Materials in MEMS: Residual Stress and Adhesion in a Micro Power Generation System

Sandia National Laboratories
Washington State University
Excellence in Engineering Fellowship

M.S. Kennedy and D.F. Bahr,

Mechanical and Materials Engineering

PO Box 642920

Washington State University

Pullman, WA 99164-2920

N.R. Moody

Hydrogen and Metallurgical Science – 8758

Sandia National Laboratories

PO Box 969 MS 9402

Livermore, CA 94551-0969

Abstract

The reliability of thin film systems is important to the continued development of microelectronic and micro-electro-mechanical systems (MEMS). The reliability of these systems is often tied to the ability of the films to remain adhered to its substrate. By measuring the amount of energy to separate the film from the substrate, researchers can predicts film lifetimes. Recent work has resulted in several different testing techniques to measure this energy including spontaneous buckling, indentation induced delamination and four point bending.

This report focuses on developing quantifiable adhesion measurements for multiple thin film systems used in MEMS and other thin film systems of interest to Sandia programs. First, methods of accurately assessing interfacial toughness using stressed overlayer methods are demonstrated using both the W/Si and Au/Si systems. For systems where fracture only occurs along the interface, such as Au/Si, the calculated fracture energies between different tests are identical if the energy put into the system is kept near the needed strain energy to cause delamination. When the energy in the system is greater than needed to cause delamination, calculated adhesion energies can increase by a factor of three due to plastic deformation.

Dependence of calculated adhesion energies on applied energy in the system was also shown when comparisons of four point bending and stressed overlayer test methods were completed on Pt/Si systems. The fracture energies of $Pt/Ti/SiO_2$ were studied using four-point bending and compressive overlayers. Varying the thickness of the Ti film from 2 to 17 nm in a $Pt/Ti/SiO_2$ system, both test methods showed an increase of adhesion energy until the nominal Ti thickness was 12nm. Then the adhesion energy began to decrease. While the trends in toughness are similar, the magnitude of the toughness values measured between the test methods is not the same, demonstrating the difficulty in extracting mode I toughness as mixed mode loading approaches mode II conditions.

Table of Contents

List of Figures

List of Tables

(Page left intentionally blank)

1 Introduction

Studies have shown that two types of fracture occur in systems with strong bonds: fracture along the interfaces and those that fracture through the layered material. When systems have strong bonds, the fracture behavior is dictated by the bulk properties of the adjoining materials. In weakly bonded materials, fracture occurs along the interface accompanied by plasticity in the adjoining metal. For ideally brittle fracture, there is a rupture of atomic bonds.

In response to this need for reliability, there have been over 200 different methods developed to measure adhesion strengths [1]. Many of these methods can only be used for specific specimen geometries, such as the particle-filled composites tensile test developed by Bai [2]. Although this test measures interface adhesion, it can only be used with rigid particles enveloped in non-viscoelastic polymers. For solid thin films on rigid substrates, the number of adhesion tests drops significantly and is further divided into tests that either qualitatively or quantitatively measure adhesion. Qualitative or semi quantitative tests, including the scotch tape test and the peel tests, give a general indication of how hard it is to separate the film from the substrate. Researchers estimate adhesion strength from the maximum external load before failure. These tests are often used in industry due to their ease of use [1], but do not actually measure the adhesion strength of the system since the energy being used to separate the interface can not be separated from the external applied load. Quantitative tests measure adhesion in terms of the energy needed to separate a specific interface area and were developed from Linear Elastic Fracture Mechanics (LEFM) principles.

In the following sections, we will examine adhesion and residual stresses in thin film systems. In addition, their importance to device reliability will be further explained.

1.1 Adhesion Energy

The term adhesion has been loosely used to define interfaces, leading to a general misnomer about what it means. Typically, adhesion is defined as good or bad where “good” is a film sticking to a substrate and “bad” is when a film does not remain fixed to the substrate. Although this works to give a general idea, the term adhesion actually refers to the amount of energy per unit area required to separate a film from its substrate along the dividing interface. As we further define adhesion, a delineation will need to be made between the true adhesion and practical adhesion of a material system.

The true work of adhesion, Γ_A, is the thermodynamic work required to create two new surfaces at the expense of the interface and is an intrinsic property of a given system that depends on the type of chemical bonding between the film and substrate. Γ_A can be calculated from

$$\Gamma_A = \gamma_f + \gamma_s - \gamma_{fs} \tag{1.1}$$

where γ_f is the surface energy of the film, γ_s is the surface energy of the substrate and γ_{fs} is interfacial energy of the two materials in contact. This true work of adhesion is a function of the types of bonds along the interface and is an intrinsic property of a film-substrate pair [1].

The first measurements of true adhesion were done for liquid-solid interfaces using contact angle methods. In this measurement system, a small liquid droplet is put on a solid and the contact angle is measured. The Young-Dupré equation relates the true work of adhesion to the contact angle, Θ, by

$$\Gamma_A = \gamma_f \left(1 + \cos\Theta\right) \tag{1.2}$$

as shown in Figure 1.1.

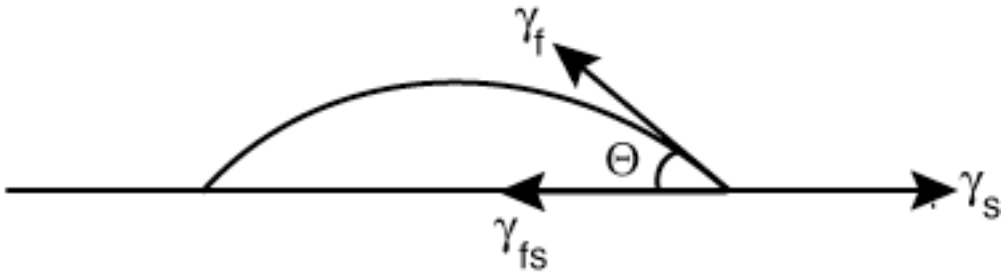

Figure 1.1: For liquid-solid interfaces, the contact angle between the droplet and solid surface may be used to calculate the adhesion energy.

For solid-solid systems, however, it is impossible to measure only a true work of adhesion. During the debonding process, there is typically an additional contribution due to the inelastic damage that occurs during the separation process [1, 3]. This inelastic damage, including plasticity and micro-cracking occurring in the regions of the substrate and film near the interface, increases the total energy needed to separate a film and substrate. This additional inelastic contribution is taken into account as follows

$$\Gamma_P = \Gamma_A + \Gamma_{inelastic} \tag{1.3}$$

where Γ_P is the total fracture energy, Γ_A is the true adhesion energy, $\Gamma_{inelastic}$ is the energy per unit area required for the inelastic deformation. $\Gamma_{inelastic}$ is actually a parameter dependent on Γ_A. This will be discussed further in chapter 3.

1.2 Surface Tension and Surface Energy

The relationship between surface tension and surface energy is described by Somorjai for one component systems [4]. When a surface is created, work is done to break bonds and remove

neighboring atoms. The reversible surface work, δW^s, needed to increase the surface area A by the amount dA under constant temperature and pressure is given by

$$\delta W^{S}_{T,P} = \gamma dA \tag{1.4}$$

where γ is the surface tension, which can be considered a pressure along the surface plane that opposes the creation of more surface. In the absence of any irreversible work, the fracture energy is equal to the total free energy of the surface. The total surface energy is equal to the specific free energy times the surface energy as shown by

$$\delta W^{S}_{T,P} = d\left(G^{S}A\right) \tag{1.5}$$

By assuming that new surface is created, the specific free energy, if independent of the surface area and the surface work, is then given by

$$\delta W^{S}_{T,P} = G^{S}dA \tag{1.6}$$

This happens when the surface is cleaved and shows that the surface tension is equal to the specific surface energy for a one-component system.

Since the true work of adhesion depends only on the types of bonds across an interface, the idealized fracture of an interface should be equal to the Griffith fracture energy. Using this link, models have been made of the decohesion of interfaces. This approach takes into account the strain energy release rate, G. When this release rate is equal to or greater than the resistance to crack propagation, R, then a crack will grow along the interface [3].

$$G \geq R \tag{1.7}$$

The resistance to crack growth is the interfacial fracture toughness of mixed mode crack growth, $\Gamma(\psi)$ [1].

This relation between the strain energy release rate and the fracture toughness defines the two considerations for interface reliability. For an interface to be reliable, the film needs to remain adhered to the substrate. This means that the stored strain energy within the film system must be less than the fracture energy, or adhesion energy.

1.3 References

[1] Volinsky AA, Moody NR, Gerberich WW. Interfacial toughness measurements for thin films on substrates. Acta Materialia 2002;50:441.

[2] Bai S-L, Wang M, Zhao X-F. Interfacial debonding behavior of a rigid particle-filled polymer composite. Composite Interfaces 2003;10:243.

[3] Hutchinson JW, Suo Z. Mixed-Mode Cracking in Layered Materials. Advances in Applied Mechanics, Vol 29 1992;29:63.

[4] Somorjai GA. Principles of Sruface Chemistry. Englewood Cliffs, NJ: Prentice-Hall, Inc., 1972.

2. Test Methods

2.1 Delamination Based Adhesion Tests

To predict the performance of film systems, industrial research groups initially developed qualitative measurement methods. These test methods, such as the tape test [1], gave engineers an idea of the relative strength of interfaces but did not give an adhesion value. Often these tests would be used to rate a film system with a pass/fail rating.

The need for quantitative methods arose from the desire to predict film adhesion under a variety of externally applied stresses and also directly compare different film systems. These quantitative measuring techniques can be subdivided into two different groups. The first group induces fracture along an interface and then estimates the adhesion energy by modeling the delamination morphology.The second group measures the crack growth rate as a function of applied load. Delamination based methods include spontaneous blisters, stressed overlayers, nanoindentation induced delamination, and scratch testing. These are discussed in section (2.2). Four-point bending, based on the rate of crack growth, will be explained in section (2.3).

2.2 Delamination Morphology Based Test Methods

2.2.1 Spontaneous Buckles and Blisters

Spontaneous blisters and buckles can be formed from compressive residual stresses in the film. The interfacial crack is driven by the stored elastic energy (residual stress). This stored energy is released when the film buckles [2]. Typical delamination morphologies include circular blisters (Figure 2.1), and straight sided (Figure 2.2) and wavy or “telephone cord” buckles (Figure 2.3). Prior work has used the models developed by Hutchinson and Suo [3] to calculate the interfacial fracture energies based on the delamination morphologies [4, 5].

The calculation of the interfacial fracture energies of the spontaneous blisters can be done using the work of Hutchinson and Suo [3] . These buckles initiate from interfacial defects and then propagate by the internal stresses in the film. Since the film has delaminated, the strain energy release rate must be equal to or greater than the fracture toughness of the interface. The interfacial fracture toughness can be calculated from estimations of the buckling stress and residual stresses of the system. These calculations are slightly different for each morphology type, but the basic process is similar. For an example, the calculations for a spontaneous blister will be shown.

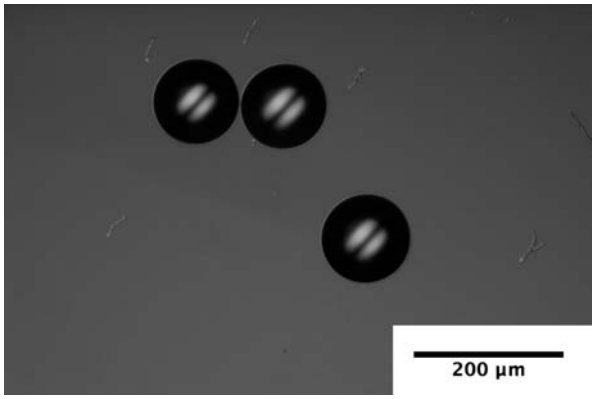

Figure 2.1: Circular blisters formed in an Au/Si system. The residual stress in the Au film was approximately 60 MPa compressive.

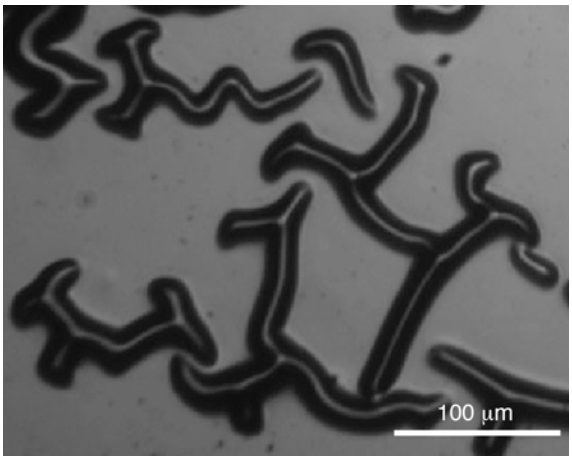

Figure 2.2: Relatively straight sided Euler buckle formed in a W/Si system.

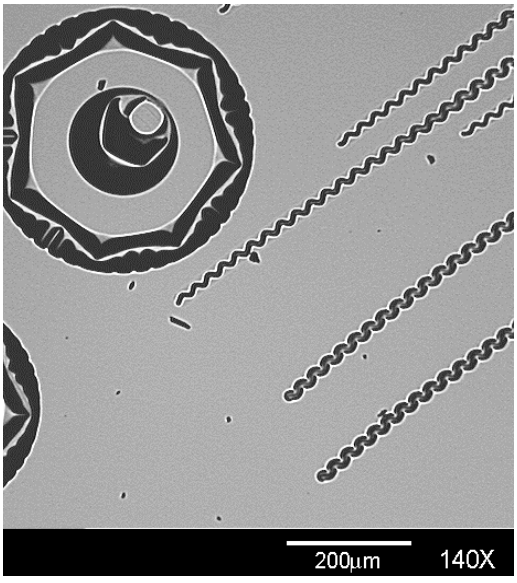

Figure 2.3: On this Figure, telephone cord blisters are evident on the upper right side. These blisters were formed on an Au/Si system.

There are two types of stresses that influence the growth of a spontaneous buckle: the critical buckling stress and the driving stress. The buckling stress is the stress required to generate delamination and the driving stress is the stress available to push out of plane deflection.

The buckling stress of a circular blister, σ_b, can be described by

$$\sigma_b = \frac{\pi^2 E}{12\left(1-\nu^2\right)}\left(\frac{h}{b}\right)^2 \tag{2.1}$$

where *h* is the thickness of the film, *b* is the radius of the induced blister, *E* is the elastic modulus of the film and ν is Poisson's ratio for the film. The delamination height, width or radius of the blister and film thickness are shown schematically on Figure 2.4 below. These dimensions are measured by atomic force microscopy (AFM) or optical microscopy.

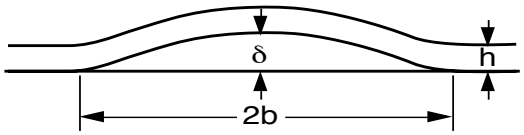

Figure 2.4: A cross sectional schematic of the dimensions of a buckle or blister.

The stress driving the delamination, σ_d, in this case the residual stress in the film, can be determined from the buckle shape. Since film delamination already occurred the driving stress is given by

$$\sigma_d = \sigma_b\left[c_1\left(\frac{\delta}{h}\right)^2 + 1\right] \tag{2.2}$$

where δ is the height of the film delamination, *h* is again the thickness of the film, and c_1 is a constant depending on Poisson's ratio, given by

$$c_1 = 0.2473\left(1+\nu\right) + 0.2231\left(1-\nu^2\right) \tag{2.3}$$

Both equation 2.1 and 2.2 are only applicable when the ratio of thickness to blister width, h/b, is much less than 1.

From the buckling and driving stresses, the fracture energies can be determined. The practical work of adhesion, $\Gamma(\psi)$, describes the amount of the energy needed for the side walls of

the buckle to arrest. The steady state fracture energy, Γ_{ss}, is the energy to propagate the buckle forward.

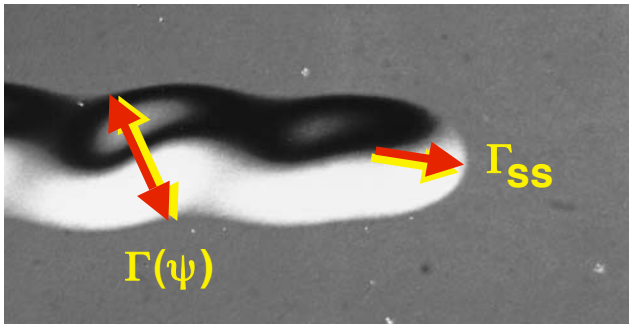

Figure 2.5: There are two fracture energies that describe the growth of a blister. The practical work of adhesion and the steady state fracture energy [6].

The practical work of adhesion is calculated from

$$\Gamma(\psi) = \left[\frac{\left(1-\nu^2\right)h}{2E}\right]\left(\sigma_d - \sigma_b\right)\left(\sigma_d + 3\sigma_b\right) \tag{2.5}$$

and the steady state energy is

$$\Gamma_{ss} = \left[\frac{\left(1-\nu^2\right)h\sigma_r^2}{2E}\right]\left(1-\frac{\sigma_b}{\sigma_d}\right)^2 \tag{2.6}$$

where the contributing factors are as described in equations (2.1) to (2.3).

Various research groups have been working on methods to explain the formation of different delamination morphologies and to determine the best methods for adhesion calculations. Although many groups agree on the film stress state to form circular blisters (equal biaxial stresses), they do not agree on the stresses required to form wavy buckles. Cleymand [7] monitored 304L stainless steel films on polycarbonate films and saw the evolution from pre-existing straight buckles to wavy buckles. During the transition, the buckles increased in width. This growth in width was shown to correlate with the release of stress in the transverse direction and indicates that this is energetically favorable for stresses along the length of the buckles. This has been put forward as the reason for the greater number of delaminations with waves versus straight sides[8]. These slight changes in stress states, however, are minimal and the models for straight-sided blisters can be applied to determine the interfacial fracture energies [5]. This work modeled Pt telephone cord blisters as both straight-sided blisters (when measured through the inflection point) and circular blisters (when measured at the curve peak) which had been

developed by Moon et al. [9]. Both models came within 15%, which is well within typical standard deviations for interfacial fracture measurements.

Normally, researchers change the residual stress in their metallic films by changing the processing pressures to increase the magnitude of compressive stress since this method has been well defined in the literature [10]. Thornton [10] showed that changing the processing pressures could also change grain size and texture. Since these changes can lead to alterations in bonding along the interface, several research groups are increasing stress though hydrogen implantation [11-13].

2.2.2 Stressed Overlayers

If a film system does not have enough compressive residual stress to delaminate, the simplest method to apply energy to the system is to add an overlayer film with a uniform compressive stress. This method enables buckle morphologies to be used to determine the adhesion energy for films under a tensile stress. Like spontaneous buckles, the adhesion energy is a function of both the driving stress and the buckling stress. The buckling stress, $\sigma_{b,}$ is a function of the moment of inertia, I_T, for the multi film system and is given by

$$\sigma_b = \frac{\mu^2}{ahb^2}\left[\frac{E_1}{\left(1-\nu_1^2\right)}\right]\left(I_T\right) \tag{2.7}$$

where h is the thickness of the film of interest and the overlayer film, b is the radius of the induced blister, E is the elastic modulus of the film, ν is Poisson's ratio for the film, and a is a geometric constant. The geometric constant drops out when evaluated with I_T. [14, 15]

I_T is determined by treating the film and overlayer as a composite beam, with moduli E_1 and E_2 and equal length. Once the composite beam is bent, the top layer elongates by factor equal to E_2/E_1. The moment of inertia of the new section, Figure 2.6, is considered to revolve around the neutral axis of the system. It is determined from the height of the neutral axis and the applications of the parallel axis theorem [14, 15].

The composite centroid $\overline{Y}$ is

$$\overline{Y} = \frac{\Sigma_k A_k y_k}{\Sigma_k\left(A_k\right)} = \frac{\overline{y_1}A_1 + \overline{y_2}A_2}{A_1 + A_2} \tag{2.8}$$

and the total transformed moment of inertia for the system is

$$I_T = \frac{1}{12}Bh_1^3 + A_1\left(\overline{Y} - \overline{y}_1\right)^2 + \frac{1}{12}n_a Bh_2^3 + A_2\left(\overline{Y} - \overline{y}_2\right)^2 \tag{2.9}$$

when the areas and centroids of the component beams are calculated as

	Material 1	Material 2
Area	$A_1=Bh_1$	$A_2=nBh_2$
Centroid	$\bar{y}_1 = h_1/2$	$\bar{y}_2 = h_1 + h_2/2$

B in these equations if the unit width, which later cancels in the critical buckling stress in when multiplied by the total transformed moment of inertia. The elastic constants are

$$E_2/\left(1-\nu_2^2\right) = n_a E_1/\left(1-\nu_1^2\right) \text{ and } E_2/\left(1-\nu_2\right) = n_b E_1/\left(1-\nu_1\right).$$

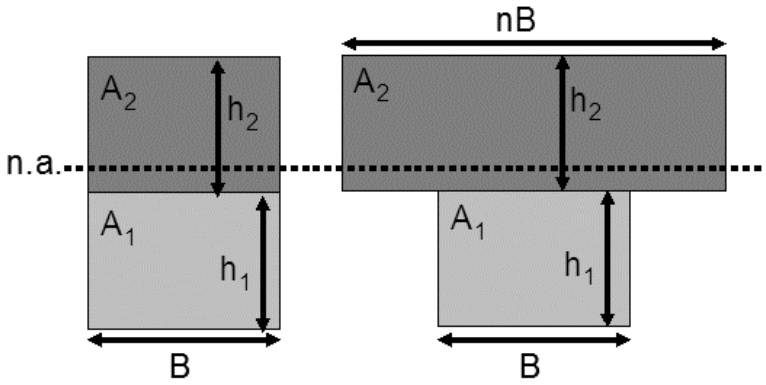

Figure 2.6: A schematic of a composite beam before (1eft) and after bending (right) [14].

The moment of inertia converges to the single layer value for one film, meaning a multi-layer film system can easily be treated as a single layer film system [14, 15]. For calculations of interfacial fracture toughness, $\Gamma(\psi)$, the modulus and Poisson's ratio values are weighted averages of the component films. Poisson's ratio is calculated as

$$\bar{\nu} = \frac{\nu_1 h_1 + \nu_2 h_2}{h_1 + h_2} \tag{2.10}$$

where $\bar{\nu}$ is thickness weighted Poisson's ratio, $h_{1,2}$ are thicknesses of each beam and $\nu_{1,2}$ are the Poisson ratios for each material. The weighted elastic modulus, $\bar{E}$ is

$$\bar{E} = \frac{E_1 h_1 + E_2 h_2}{h_1 + h_2} \tag{2.11}$$

and $E_{1,2}$ is the elastic modulus for material 1 and 2.

2.2.3 Indentation Induced Delamination

Inducing delamination with an indenter was shown to be an efficient way to induce delamination by Marshall [16] when there is not enough driving energy from residual stresses or overlayers. A conical indenter is driven perpendicularly into the film causing a radial expansion of the film that can initiate cracking along the interface and also drive propagation of that crack. To relieve the strain energy, the film can either buckle as the indenter tip is being driven into the film during loading or as the tip is being removed from the sample. Marshall [16] used these steps to determine the interfacial fracture toughness of a film using indentation techniques as shown in Figure 2.7.

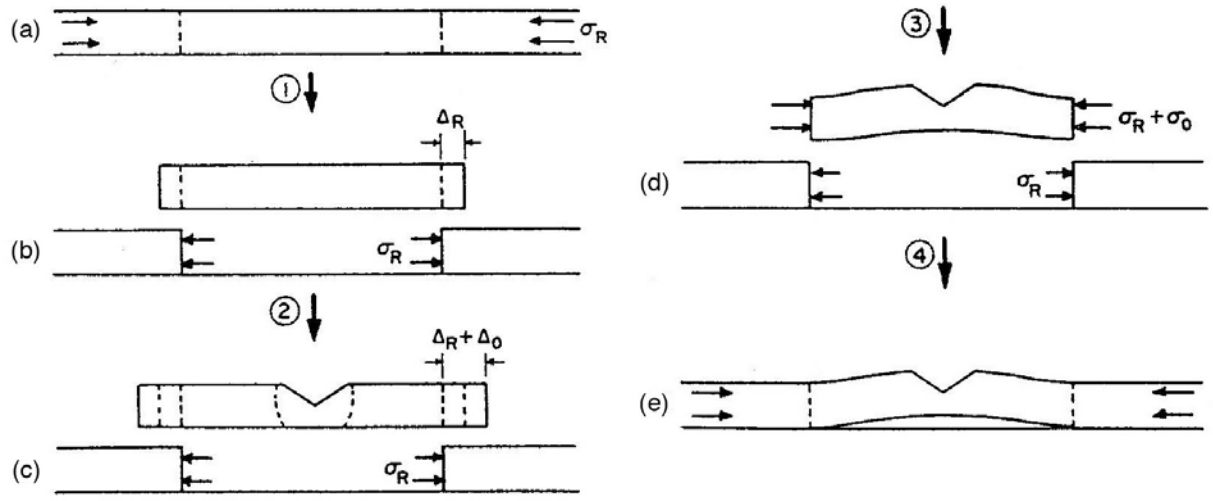

Figure 2.7: Marshall and Evans [16] used these steps to determine the interfacial fracture toughness of a film using indentation techniques.

To determine the interfacial fracture energy, the crack is assumed to form directly under the indenter tip [17]. The total strain energy to create a blister in the film above the interfacial crack is modeled by assuming the fracture is a clamped circular plate, where the indent is kept within the film. Like the stressed overlayer method, the fracture energy, $\Gamma(\psi)$, takes into account the critical buckling stress, σ_b, the driving stress, σ_d, and the indentation stress, σ_I. The indentation stress, the stress required to recompress the section, can be calculated with the following equation

$$\sigma_I = \frac{V_I E}{2\pi h b^2 (1-\nu)} \tag{2.12}$$

where V_I is the volume of the residual indentation. The volume is estimated from the indentation depth and the area function of the indenter tip. The buckling stress, σ_b,is given by

$$\sigma_b = \frac{\mu^2 h^2 E_f}{12a^2\left(1-\nu_f\right)} \tag{2.13}$$

where μ is depends on the boundary conditions of the delamination.

The interfacial fracture energy, $\Gamma(\psi)$, is then given by

$$\Gamma\left(\psi\right) = \frac{h\sigma_I^2\left(1-\nu^2\right)}{2E} + \left(1-\alpha\right)\frac{h\sigma_d^2\left(1-\nu\right)}{E} + \left(1-\alpha\right)\frac{h\left(\sigma_I-\sigma_b\right)^2\left(1-\nu\right)}{E} \tag{2.14}$$

where α, is the slope of the buckling load versus the edge displacement defined as

$$\alpha=1/[1+0.902(1-\nu)] \tag{2.15}$$

This test has been modified by adding a stressed overlayer to the system of interest before delamination by Kriese [14]. The overlayer was able to prevent plastic flow of the underlying film in the verticle direction and provide extra driving force for delamination.

2.2.4 Scratch Testing

Another way of applying energy is through scratch testing were the load is applied both laterally as well as the normally with an indenter tip. The vertical load is continually increased until delamination of the film.

There are several ways of determining the adhesion energy. When the delamination is uniform on both sides of the scratch, Moody et al. [18M] have shown that a circular blister analysis can be used. The test consists of drawing a stylus or indenter with a known radius of curvature over a film or coating under increasing vertical loads. Resultant scratches are then observed under an optical or scanning electron microscope in order to estimate the minimum or critical load required delaminating the film. Circular film delaminations are modeled like circular blisters.

2.3 Four-point Bending

Using specific sample geometry and loading configurations, the four-point bending test technique measures the critical load sufficient for crack growth along an interface that can then be used to calculate the sample's strain energy release rate required for crack growth. At this critical load where crack growth occurs, the strain energy release rate equals the interfacial fracture energy. This experimental technique was derived by originally Charalambides for laminate composites [19, 20] and then further developed to measure the adhesion of thin films for microelectronics by Dauskardt et al. [21-37].

In this test, the interface of interest is bonded between two elastic substrates. The load then is applied to the bulk material sandwiching the interface, making it easy to control the interface crack growth. The sample is loaded as shown in Figure 2.8.

The bending moment increases with load, and a pre-crack initiates from the notch to the interface of interest. During testing; the load is monitored while the displacement rate of the crosshead is kept constant, Figure 2.9. The initial linear part of the load-displacement results from elastic loading of the composite beam, storing strain energy in the massive elastic substrates. At the critical load, the strain energy available for fracture becomes larger than the fracture resistance of the interface and results in a load plateau and debond extension. By using beam mechanics, and determining the critical load at which a displacement plateau is seen, the critical strain energy release rate can be determined. The resulting interface fracture energy is a function of the critical value of the applied strain energy release rate (G) as follows

$$G = \frac{21(1-\nu^2)M^2}{4Eb^2h^3} = \frac{21(1-\nu^2)P^2l^2}{16Eb^2h^3} \tag{2.16}$$

where the bending moment is given by M=P*l*/2, with P being the load and *l* the spacing between the inner and the outer loading lines, b is the beam width, h is the half thickness, and E and v are the elastic modulus and Poisson's ratio of the bulk substrate respectively.

It is important to note that only when the crack tip is sufficiently away from the vertical precrack (a>2h), the strain energy release rate is independent of the crack length.

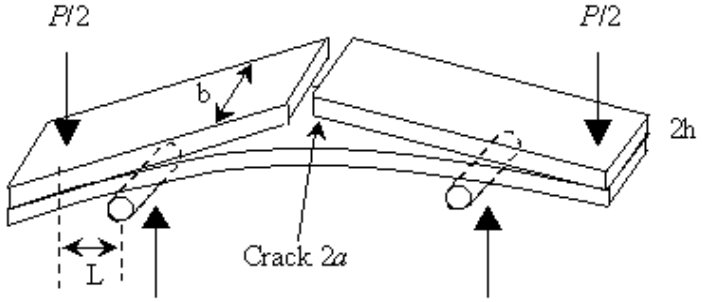

Figure 2.8: Four-point bend specimen with a crack length of 2a. [38]

Unlike spontaneous, stressed overlayer or indentation-induced delamination, the mode mixity of the loading is constant, ~43°. This is an attractive technique since the loading mode mixity represents an almost equal amount of shear to normal stresses. Elastic curvature due to the residual stress in the film will only make a small contribution to the measured strain energy release rate.

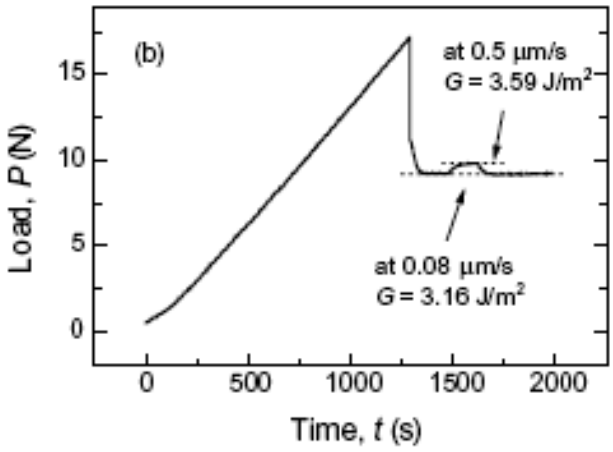

Figure 2.9: A load displacement curve showing typical trends during a four-point bend test [37].

The precision of four-point bend test results is highly dependant on sample preparation. Parameters such as substrate material, bond type and thickness, notch depth and polishing all influence the calculated interfacial fracture energy.

2.4 Comparing Adhesion Values Between Tests

Films may fail under a variety of stresses ranging from all normal stresses, to a combination of shear and normal stresses, to pure shear stresses. Each test technique measures the adhesion energy corresponding to a different ratio of shear to normal stresses and is described by the phase angle of loading or mode mixity, ψ. The phase angle of loading is a ratio of the mode II to mode I stress intensities as follows

$$\psi = \tan^{-1}\left(\frac{k_{II}}{k_I}\right) \tag{2.17}$$

where k_{II} and k_I are the stress intensity factors for mode II and mode I respectively. As shown in Figure 2.10, this ratio of stresses influences the magnitude of energy dissipation needed for fracture. When the mode mixity is 0^o , fracture is caused by all normal forces and is often referred to as the mode I fracture energy. When the fracture is caused by pure shear forces, $\pm 90^o$, it is a mode II failure. Most measured values consist of mixed mode I normal and mode II shear contributions. The mode I contribution is the value that is of interest because it is a measure of adhesion and toughness. The criterion most often used to determine the normal mode I contributions from measured mixed mode values is,

$$\Gamma_I = \frac{\Gamma(\psi)}{\left[1 + \tan^2\left((1-\lambda)\psi\right)\right]} \tag{2.18}$$

where λ is an empirical material constant that adjusts the influence of the mode II contribution [3]. The values of λ range from 0 to 1 with 0 depending on only mode I component and 1 being ideally brittle. For most all of the systems used in this study, λ will be approximately 0.3.

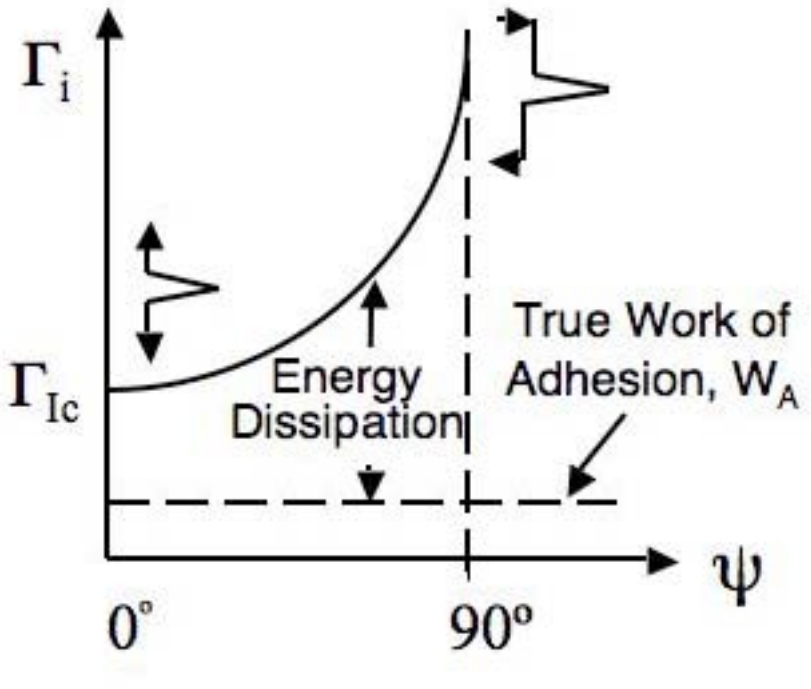

Figure 2.10: This shows the relationship between the mode mixity and the interfacial adhesion energy [6].

2.5 References

[1] Goh LLN, Toh SL, Chooi SYM, Tay TE. Adhesion measurement of thin films to a porous low dielectric constant film using a modified tape test. Journal of Adhesion Science and Technology 2002;16:729.

[2] Thouless MD, Hutchinson JW, Liniger EG. Plane-strain, buckling-driven delamination of thin films: model experiments and mode-II fracture. Acta Metallurgica et Materialia 1992;40:2639.

[3] Hutchinson JW, Suo Z. Mixed-Mode Cracking in Layered Materials. Advances in Applied Mechanics, Vol 29 1992;29:63.

[4] Branger V, Coupeau C, Goudeau P, Boubeker B, Badawi KF, Grilhe J. Atomic force microscopy analysis of buckling phenomena in metallic thin films on substrates. Journal of Materials Science Letters 2000;19:353.

[5] Cordill MJ, Bahr DF, Moody NR, Gerberich WW. Adhesion measurements using telephone cord buckles. Materials Science & Engineering A (Structural Materials: Properties, Microstructure and Processing) 2007;443:150.
[6] Volinsky AA, DF Bahr, MD Kriese, NR Moody, W Gerberich. Comprehensive Structural Integrity vol. 8.13. p.453.
[7] Colin J, Cleymand F, Coupeau C, Grilhe J. Worm-like delamination patterns of thin stainless steel films on polycarbonate substrates. Philosophical Magazine A: Physics of Condensed Matter, Structure, Defects and Mechanical Properties 2000;80:2559.
[8] Cleymand F, Coupeau C, Grilhe J. Atomic force microscopy investigation of buckling patterns of nickel thin films on polycarbonate substrates. Philosophical Magazine Letters 2002;82:477.
[9] Moon MW, Jensen HM, Hutchinson JW, Oh KH, Evans AG. The characterization of telephone cord buckling of compressed thin films on substrates. Journal of the Mechanics and Physics of Solids 2002;50:2355.
[10] Thornton JA, Hoffman DW. Stress-related effects in thin films. Thin Solid Films 1989;171:5.
[11] Pundt A, Pekarski P. Buckling of thin niobium-films on polycarbonate substrates upon hydrogen loading. Scripta Materialia 2003;48:419.
[12] Pundt A, Nikitin E, Pekarski P, Kirchheim R. Adhesion energy between metal films and polymers obtained by studying buckling induced by hydrogen. Acta Materialia 2004;52:1579.
[13] Nikitin E, Kirchheim R, Pundt A. Determination of adhesion energies by means of hydrogen loading. Journal of Alloys and Compounds 2005;404-406:477.
[14] Kriese MD, Gerberich WW, Moody NR. Quantitative adhesion measures of multilayer films: Part I. Indentation mechanics. Journal of Materials Research 1999;14:3007.
[15] Kriese MD, Gerberich WW, Moody NR. Quantitative adhesion measures of multilayer films: Part II. Indentation of W/Cu, W/W, Cr/W. Journal of Materials Research 1999;14:3019.
[16] Marshall DB, Evans AG. Measurement od Adherence of Residually stressed Thin Films by Indentation: I. Mechanics of Interface Delamination Journal of Applied Physics 1984;56:2632.
[17] Volinsky AA, Tymiak NI, Kriese MD, Gerberich WW, Hutchinson JW. Quantitative modeling and measurement of copper thin film adhesion. Materials Research Society Symposium - Proceedings 1999;539:277.
[18] Moody NR, Hwang RQ, Venkataraman S, Angelo JE, Gerberich WW, Adhesion and Fracture of Tantalum Nitride Thin Films, *Acta Materialia* 1998;46:585.
[19] Charalambides PG, Evans AG. Debonding properties of residually stressed brittle-matrix composites. Journal of the American Ceramic Society 1989;72:746.
[20] Sbaizero O, Charalambides PG, Evans AG. Delamination cracking in a laminated ceramic-matrix composite. Journal of the American Ceramic Society 1990;73:1936.
[21] Zhenjiang C, Dixit G, Li-Qun X, Demos A, Kim BH, Witty D, M'Saad H, Dauskardt RH. Benchmarking four point bend adhesion testing: the effect of test parameters on adhesion energy. AIP Conference Proceedings 2005:507.
[22] Gage DM, Kyunghoon K, Litteken CS, Dauskardt RH. Effects of friction and loading parameters on four-point bend adhesion measurements of low-k thin film interconnect structures. Proceedings of the IEEE 2005 International Interconnect Technology Conference (IEEE Cat. No. 05TH8780) 2005:42.
[23] Litteken CS, Strohband S, Dauskardt RH. Residual stress effects on plastic deformation and interfacial fracture in thin-film structures. Acta Materialia 2005;53:1955.

[24] Lee A, Litteken CS, Dauskardt RH, Nix WD. Comparison of the telephone cord delamination method for measuring interfacial adhesion with the four-point bending method. Acta Materialia 2005;53:609.
[25] Guyer EP, Dauskardt RH. Effect of aqueous solution chemistry on the accelerated cracking of lithographically patterned arrays of copper and nanoporous thin-films. Materials, Technology and Reliability for Advanced Interconnects and Low-k Dielectrics-2004 (Materials Research Society Symposium Vol.812) 2004:303.
[26] Renuart ED, Fitzgerald AM, Kenny TW, Dauskardt RH. Fatigue crack growth in micro-machined single-crystal silicon. Journal of Materials Research 2004;19:2635.
[27] Sharratt BM, Dauskardt RH. Debonding under fatigue loading at polymer/inorganic interfaces. Nanoscale Materials and Modeling-Relations Among Processing, Microstructure and Mechanical Properties (Materials Research Society Symposium Proceedings Vol.821) 2004:363.
[28] Guyer EP, Dauskardt RH. Electrical technique for monitoring crack growth in thin-film fracture mechanics specimens. Journal of Materials Research 2004;19:3139.
[29] Litteken C, Dauskardt R, Scherban T, Xu G, Leu J, Gracias D, Sun B. Interfacial adhesion of thin-film patterned interconnect structures. Proceedings of the IEEE 2003 International Interconnect Technology Conference (Cat. No.03TH8695) 2003:168.
[30] Nagarajan K, Dauskardt RH. Adhesion and reliability of underfill/substrate interfaces in flipchip BGA packages: metrology and characterization. Seventh Annual 2002 Proceedings. Pan Pacific Microelectronics Symposium 2002:251.
[31] Strohband S, Dauskardt RH. Interface separation in residually-stressed thin-film structures. Interface Science 2003;11:309.
[32] Wang LC, Dauskardt RH. Effect of moisture and graded-layer mechanical properties on deformation and interfacial adhesion. Mechanical Properties Derived from Nanostructuring Materials. Symposium. (Mater. Res. Soc. Symposium Proceedings Vol. 778) 2003:227.
[33] Strohband S, Dauskardt RH. Multi-scale simulations of interfacial fracture of nanoscale thin-film structures: effect of length scales and residual stresses. Mechanical Properties Derived from Nanostructuring Materials. Symposium. (Mater. Res. Soc. Symposium Proceedings Vol. 778) 2003:303.
[34] Litteken CS, Dauskardt RH. Adhesion of polymer thin-films and patterned lines. International Journal of Fracture 2003;120:475.
[35] Snodgrass JM, Pantelidis D, Jenkins ML, Bravman JC, Dauskardt RH. Subcritical debonding of polymer/silica interfaces under monotonic and cyclic loading. Acta Materialia 2002;50:2395.
[36] Ma Q, Bumgarner J, Fujimoto H, Lane M, Dauskardt RH. Adhesion measurement of interfaces in multilayer interconnect structures. Materials Reliability in Microelectronics VII. Symposium 1997:3.
[37] Dauskardt RH, Lane M, Ma Q, Krishna N. Adhesion and debonding of multi-layer thin film structures. Engineering Fracture Mechanics 1998;61:141.
[38] Volinsky AA, Moody NR, Gerberich WW. Interfacial toughness measurements for thin films on substrates. Acta Materialia 2002;50:441.

3. Comparison of Delamination Test Methods

3.1 Measurement Consistency

The fracture test systems outlined in section 2 can be used to measure the adhesion energy of films with either compressive or tensile residual stresses. Each test system has limitations and can not be used on all film systems. For compressive films that have already started to delaminate, four-point bending is unable to measure the film's adhesion since subsequent processing would lift the film off completely. The stressed overlayer method only works on film systems where the adhesion strength of the overlayer-film is greater than the film-substrate. Since no universal method can be used for all films, a comparison of these methods for identical systems is desired. This would allow researchers to directly compare the Mode I values for a variety of test systems using the most appropriate fracture technique.

This chapter will focus on determining adhesion energy using different delamination techniques including scratch, indentation and spontaneous overlayers. As explained in the previous chapter, the measured adhesion energy can be affected by contributions including chemistry, texture, plasticity and roughness. Of these parameters, plasticity can be controlled through optimization of the test method. Often, only one of these test techniques is used. In addition, there is a need to understand the constraints and applicability of each method to metal-dielectric systems. Comparisons of the delamination based test methods will be focused upon in this chapter. These techniques will be applied and compared in two systems: W/Si and Au/Si.

3.2 W/Si Fracture Energies

W/SiO_2 was used to study the sensitivity of measurement techniques to additional inelastic deformation. This system was chosen since it has been well characterized [1-3] and can easily be deposited with DC magnetron sputtering to have high compressive stresses. This study deposited compressive W films and compared the resulting fracture energies from spontaneous blisters, scratch testing and indentation induced delamination.

3.2.1 Experimental Procedures

A thin 250 nm compressive W film was deposited using DC magnetron sputtering onto native oxide formed on a (100) Si wafer. The (100) Si was cleaned before film deposition using an acetone/IPA/H_2O/acetone/IPA rinse process. A Nanoindenter XP system with a 1μm radius of curvature conical indenter tip (with an included angle of 90º) was used to apply a loads of 25 mN, 50 mN, 100 mN, and 200 mN each for 10 indentations. Scratch tests were done at a rate of 0.5 μm/sec along a 200 μm length in the lateral direction to a maximum normal load of 100mN . Delamination morphologies were measured with an Autoprobe CP Scanning Probe Microscope in the atomic force microscopy (AFM) mode.

3.2.2 Results

Delamination morphologies formed from these tests are shown in Figure 3.1. This optical image shows the delamination morphologies after indention and scratch testing as well as spontaneous buckling of the film. Optical examination indicate that both the scratch and indentation tests exhibit through-thickness radial cracking in the film. AFM images, Figure 3.2, show that only the scratch tests exhibit cracking.

The adhesion energies given in Table 1, show that energies for the indentation induced blisters and scratch blisters are lower than for spontaneous buckles. All of these calculations were made using the equations described in section 2 and the following values: ν_{film}= 0.39, E_{film}= 400 GPa.

The differences between these calculated energies is due to inelastic deformation not accounted for in the models. Cracking occurred during scratch testing and pile up during indentation. Although cracking should theoretically raise the calculated adhesion energy, the pile-up exaggerates the height of the film delamination, making the calculated adhesion energy lower. Radial cracking is suspected to reduce the hoop stress and constraint in the film. This then allows the film to curl away from the substrate.

Another area for errors in measurement of the adhesion energy is associated with the ratio of the blister to indentation radius. A small ratio indicates a large contribution of indentation stress to the stress for buckle formation and an overestimation of adhesion energy.

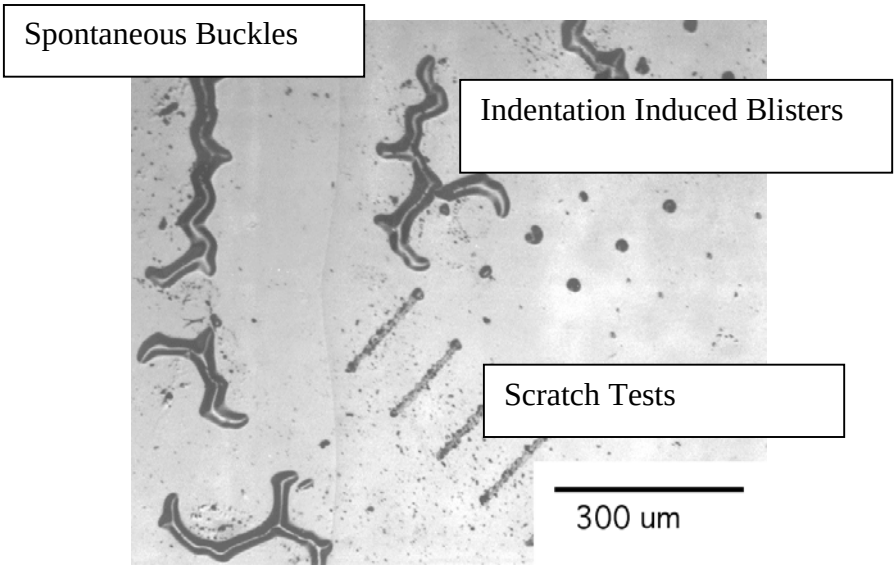

Figure 3.1: Delamination of W/SiO_2 by scratch testing, indentation and residual stresses in the deposited film.

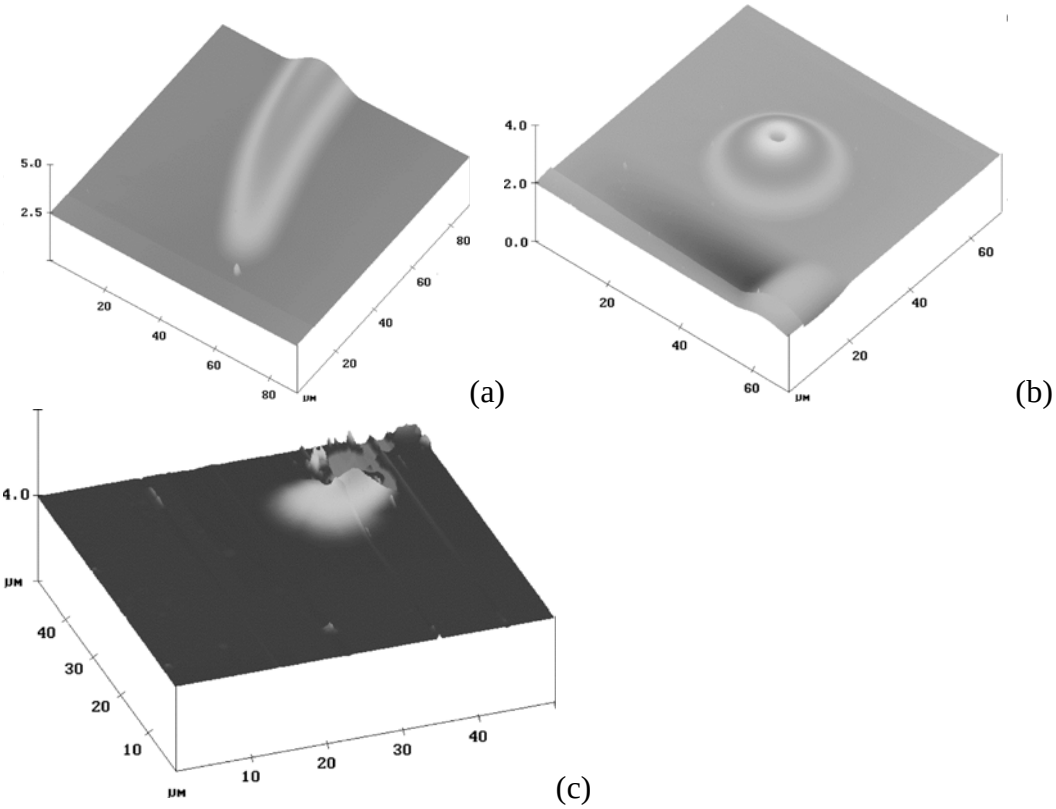

Figure 3.2 (a-c): AFM images of delamination morphologies from testing of W/SiO_2 by scratch testing (c), indentation (b) and residual stresses (a) in the deposited film.

	Interfacial Fracture Energy (J/m^2)
Spontaneous Euler Buckles	0.63±0.17
Indentation Induced Blisters	0.17±0.02
Scratch Tests	0.24

Table 3.1: The calculated mode I adhesion energies for W/SiO_2. The standard deviations were calculated using a sample set of ten tests for both the spontaneous and indentation induced blisters.

3.3 Au/Si Fracture Energies

The most common Au film system studied is Au/sapphire [4] as the Au/sapphire system does not form any interphase regions. On the otherhand, the Au/SiO_2 is frequently used in MEMS devices, such as MEMS mirrors. However, it is also noted for diffusion between the Au and Si. For this reason we chose to study the Au/SiO_2 system.

3.3.1 Experimental Procedures

150nm Au films were deposited onto native SiO_2 on (100) Si wafers by DC magnetron sputtering at Sandia National Laboratories. The wafers were then diced into small sections and W overlayers with varying thickness (220 nm, 250 nm, and 330 nm) were deposited on the diced substrates. The Au films were cleaned before film deposition using an acetone/IPA/H_2O/acetone/IPA rinse process. Circular blister delamination morphologies were measured with an Autoprobe CP Scanning Probe Microscope in the atomic force microscopy (AFM) mode.

3.3.2 Results

The interfacial energies for the Au/native SiO_2 driven by different W overlayers are shown in Table 3.2. In section 2, several studies had shown a correlation between film thickness and measured fracture energies. This study does not show the same trend. This may be due to the different deposition conditions of the W, resulting in different film textures.

Sample	Practical (J/m^2)	Mode I (J/m^2)	Residual Stress in the System (MPa)	Phase Angle (Degrees)	W Thickness (nm)
Au with W	1.1	0.2	1600	-85	250
Au with W	2.0	0.4	1300	-75	400
Au with W	0.24	0.09	600	-70	330

Table 3.2: This table shows both the mode I and the practical interfacial fracture energies for three different W/Au/SiO_2 systems.

3.4 Conclusions

Cracking within the film and substrate can lead to errors in the calculation of fracture energies. This generally results in an overestimation of energies. On the other hand, our results with the W/ SiO_2 system show that pile-up exaggerates buckle height and can lead to an underestimation of fracture energies. When both cracking and pile up are minimized, the calculated fracture energies using different delamination models were similar as shown with the Au/SiO_2 system. These limited studies clearly show that the calculated fracture energies can vary significantly for identical systems depending on test mode or the magnitude of driving stresses: Au/SiO_2: .09-.40 J/m^2 and W/SiO_2: 0.17-0.63 J/m^2. This variation indicates the range in values which may be expected when selecting different test methods.

3.5 References

[1] Cordill MJ, Bahr DF, Moody NR, Gerberich WW. Recent developments in thin film adhesion measurement. IEEE Transactions on Device and Materials Reliability 2004;4:163.
[2] Cordill MJ, Bahr DF, Moody NR, Gerberich WW. Adhesion measurements using telephone cord buckles. Materials Science & Engineering A (Structural Materials: Properties, Microstructure and Processing) 2007;443:150.
[3] Cordill MJ, Moody NR, Bahr DF. Adhesion of thin ductile films using stressed overlayers and nanoindentation. vol. 750. Boston, MA, United States: Materials Research Society, 2002. p.33.
[4] A. A. Volinsky DFB, M. D. Kriese, N. R. Moody, W. Gerberich. Comprehensive Structural Integrity vol. 8.13. p.453.

4. Stressed Overlayers and Four Point Bending

4.1 Pt-Ti-SiO_2 System

Most adhesion studies have examined the interfacial fracture energies of systems with uniform dimension, interfacial chemistries and stresses. There is also a need to characterize the interfacial fracture energies of non-uniform systems created by contamination or deposition of discontinuous films. Schneider et al. showed that the interfacial toughness between Al and sapphire decreases when 5-20 nm of carbon is sputtered on the sapphire substrate prior to deposition of Al [1]. Kennedy et al. [2] have shown that altering surface chemistry through discontinuous polymer patterning significantly weakens the tungsten-SiO_2 interface. Pt films are of particular interest as they have often been used as bottom electrodes for PZT (lead zirconate titanate) films because of their stability in high-temperature oxidizing atmospheres. The addition of a Ti interlayer has been used to improve the adhesion of the Pt to oxides [3]. This layer is susceptible to changes in chemistry during high temperature processing. When a critical temperature and time combination is reached, evolution of the Pt/Ti interface typically turns into a Pt/TiO_2, with the O diffusing into the titanium layer from the substrate [4]. Although a few isolated measurements of the interfacial fracture energy have been made of fully aged Pt/TiO_2 systems, no study has looked at the progression of interfacial fracture energy with respect to non uniform changes in interface chemistry. Another reason for studying non-uniform interfaces is to look at growth mechanisms of the thin films. As many films deposit, they form islands prior to complete coverage [5, 6]. The coverage of the Ti has been shown to be non uniform on oxides in previous studies [7, 8]. In order to predict the evolution of an interface's fracture energy over a device lifetime, a better understanding of non-uniform interface fracture energy must be made. This study uses DC magnetron sputtering to deposit a non uniform Ti interlayer in a Pt/Ti/SiO_2 system to explore the interface fracture energy with increasing Ti thickness.

4.2 Buckling Measurements of Interfacial Toughness in Pt-Ti-SiO_2

As the deposition time of Ti is increased to deposit nominal thicknesses of 1, 3, 6, 12 and 17 nm Ti layers, two results can occur. If the Ti forms layer by layer, there should be a sharp transition between measured adhesion energies with no titanium interlayer, i.e. the Pt/SiO_2 system, to values nearing a known uniform coverage of the Ti in the Pt/Ti/SiO_2 system. If island growth occurs, however, there will not be a sharp transition between adhesion values once the Ti interlayer is deposited. Instead, a gradual increase of adhesion values typical for the Pt/SiO_2 to values typical of the Pt/Ti/SiO_2 system was observed, similar to the rule of mixtures behavior exhibited by the W/SiO_2 system.

A typical sample set up for each of the Ti interlayers is shown in Figure 4.1, where the silicon wafer was sectioned into four quadrants: SiO_2 (lower right), W/SiO_2 (lower left), Pt/Ti/SiO_2 (upper left), and W/Pt/Ti/SiO_2 (upper right). This setup allowed for ease of measuring film thicknesses and quick measurement of W residual stress. It should be noted that this

patterning of the samples did not impose a new mechanism of delamination growth. Delamination only occurred when the residual stress in the W was large enough to cause delamination at the interface containing the SiO_2. Figure 4.2 shows that the buckles stopped along the interface between the W/SiO_2 and $W/Pt/Ti/SiO_2$ systems when the residual stress of the W was not large enough to cause crack growth between the Ti and SiO_2. If the residual stress was high enough to cause delaminations in both systems to occur, a noted transition in the size and shape of the buckles formed between the regions of high adhesion, Ti/SiO_2, and poor adhesion, Pt/SiO_2. A typical image showing this transition is shown in Figure 4.3.

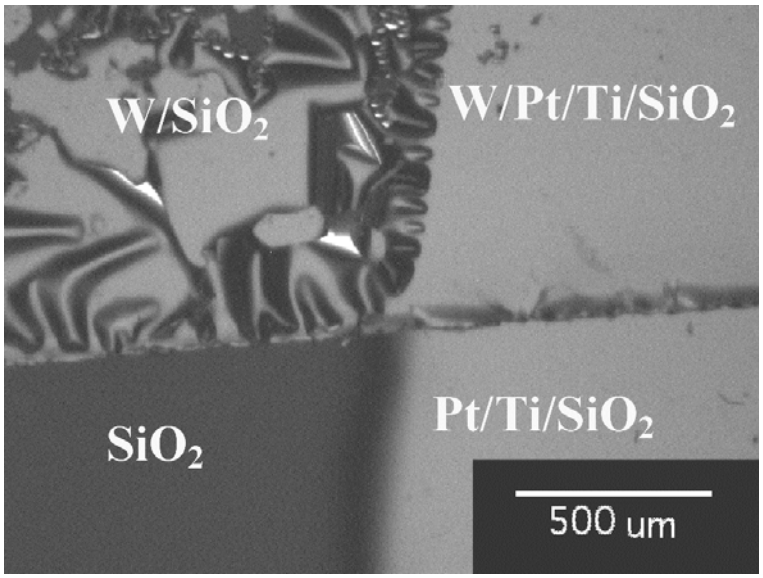

Figure 4.1: A typical sample design for measuring the film thickness and interfacial energy of $Pt/Ti/SiO_2$.

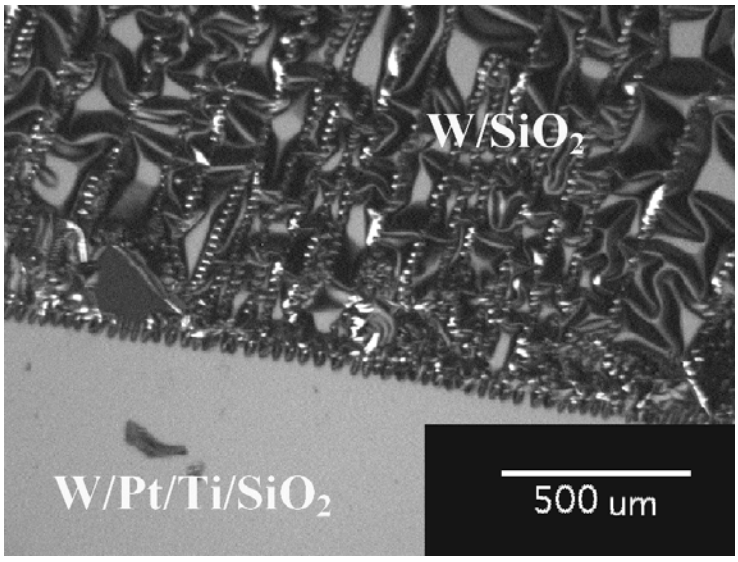

Figure 4.2: Film delamination only occurred once the W compressive residual stress was enough to delaminate a film system.

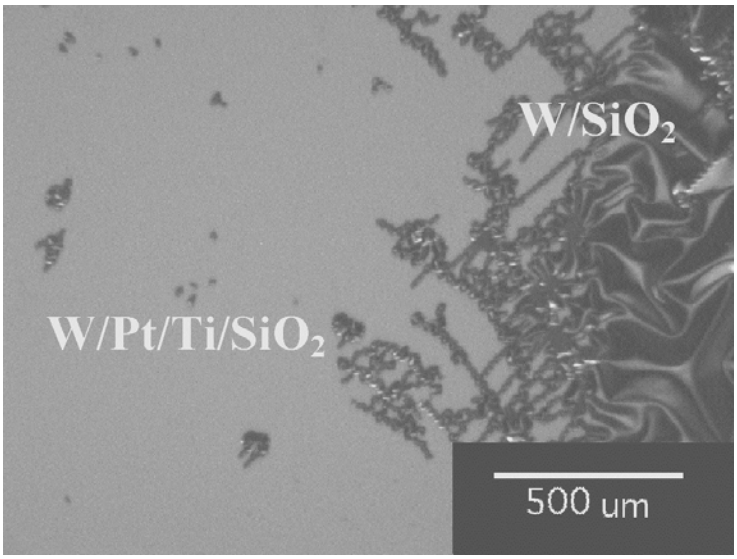

Figure 4.3: In this film system, the W had a high enough stress to delaminate both the Ti/SiO_2 and Pt/SiO_2 systems.

Using the equations described in section 2, the buckling stress, driving stress, phase angle of loading, and practical and mode I values of adhesion energies for these systems were found. The driving stress for each system was slightly different due to increases in W thicknesses and also tensile stresses within the Pt films. For all delaminations, however, the phase angle was around -89°. This makes direct comparison of the practical work of adhesion possible. The averages and standard deviations were calculated from the interfacial fracture energies of six different buckles. The measured practical work of adhesion for mixed mode failure of the Pt/SiO_2 interface was 10 J/m^2 and the measured value of the Pt/17 nmTi/SiO_2 interface was 41 J/m^2. These values were both within previously reported ranges. The measured values for Ti at 1, 3 and 6 nm were 26, 40 and 62 J/m^2 respectively, and are plotted with standard deviation of the measurements in Figure 4.4. Films with 12nm Ti layers never delaminated using this method.

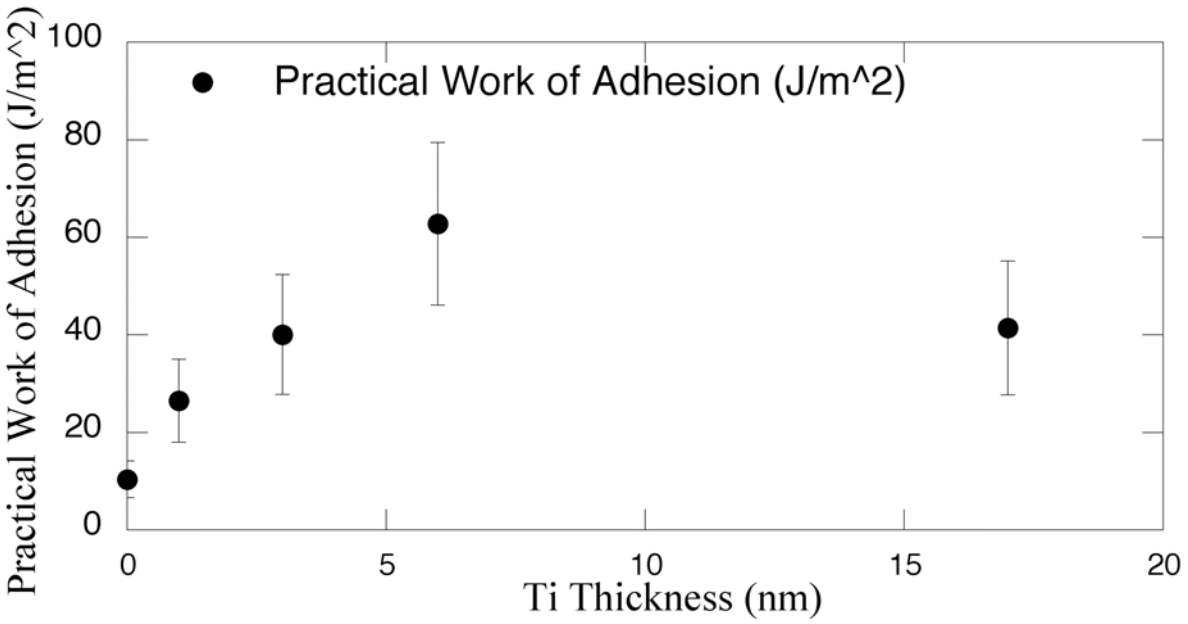

Figure 4.4: As the percentage of the interface is covered by Ti, the interfacial fracture energy increases.

4.3 Four Point Bend Tests of the Pt-Ti-SiO_2 System

4.3.1 Substrate Preparation

For four-point bend samples, a silicon dioxide passivation layer was grown to a thickness of 1μm on both sides of polished (100) Si wafers by a wet thermal process. The original Si wafers had a thickness of 420μm. To etch dice lines, the oxide on the front side of the wafer was first patterned by positive photolithography. The oxidized wafer was spin coated with hexamethyldisilazane (HMDS), which served as an adhesion promoter at 3000 rpm for 30 seconds. Then, photoresist AZ5214-EIR was spun at the same conditions and underwent a soft bake on a hot plate at 110°C. The mask, shown in Figure 4.8, and wafer are then aligned and exposed to a UV light source for 12 seconds. The exposed regions were dissolved away using a 4:1 mixture of DI water and AZ400K developer. Once the oxide was etched away in BOE (buffered oxide etchant), the AZ400K developer was rinsed off using acetone. The remaining oxide acted as etch stop for the anisotropic wet etch EDP (ethylene–diamine–pyrocatechol). After etching dice lines, the wet oxide was stripped off the entire wafer using BOE and then regrown to a thickness of 250 nm.

The specimens for four-point bend experiments were 3.81 mm wide and the spans used for experiments were 25mm and 40mm. Film systems were bonded with a low-temperature epoxy (Allied High Tech EpoxyBond 100) and cured at 150°C for 45 minutes. Notches were scribed into the sample and notched by EDP etching.

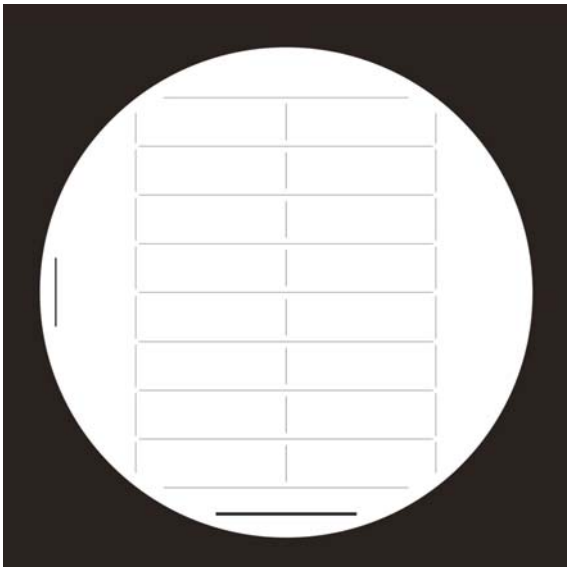

Figure 4.5a: Mask pattern to fabricate the top Si beams that sandwich the interface of interest during four-point bending. Each beam is 3.81 mm wide and the notches are 2um deep.

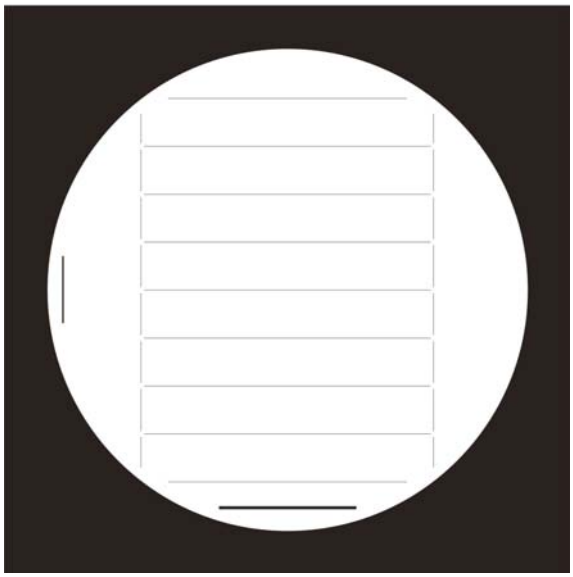

Figure 4.5b: Mask pattern to fabricate the back Si beams that sandwich the interface of interest during four-point bending.

The four-point bend test system was fabricated at Washington State University, and is described in the PhD thesis of M.S. Kennedy (2007). Complete schematics of the system are beyond the scope of this report. The displacement rate of the crosshead was 0.1 μm/s. The interfacial debonds from five different beams were propagated along the selected interfaces. Since a thick thermal oxide was grown, a visual inspection of the surface was made to determine that the cracks grew along the metal/SiO_2 interfaces and not the metal/epoxy interfaces.

4.3.2 Four-Point Bend Results

Most four-point bend studies use wafer saws to dice Si beams [9-12]. Following their example, beams were diced and the edges mechanically polished. For these samples, notching was either done using a diamond scribe or a diamond saw. However, all samples failed catastrophically at low loads. An example of this catastrophic failure is shown in Figure 4.9. This was caused by the surface damage of the Si during cutting with wafer saw, shown in Figure 4.10. To decrease the surface damage, a new technique of etching dice lines and notches using EDP was developed. This method resulted in smooth sidewalls, Figure 4.11.

Five samples of each specimen were loaded until plateaus occurred. Identification of the interface through which the crack propagated was verified using optical microscopy since the coloration of each layer was distinct. Figure 4.12 shows that the critical load at which crack extension occurred increased when the Ti interlayer thickness increased from 6nm to 12nm, then

decreased as thickness increased to 20nm. The load-displacement curves varied between samples of the same compositions, Figure 4.13. The initial plateau loads were first averaged over the first 20μm for each sample. The average of five samples was then used to calculate the fracture energy using equation 2.13.

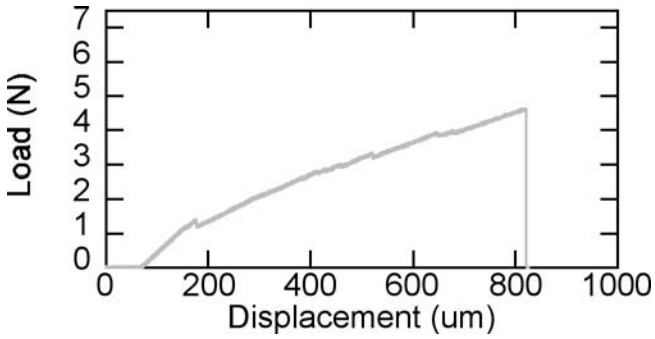

Figure 4.6: Catastrophic failure of Pt sandwich specimen. This failure was due to roughening of the Si surface and introduction of flaws during dicing.

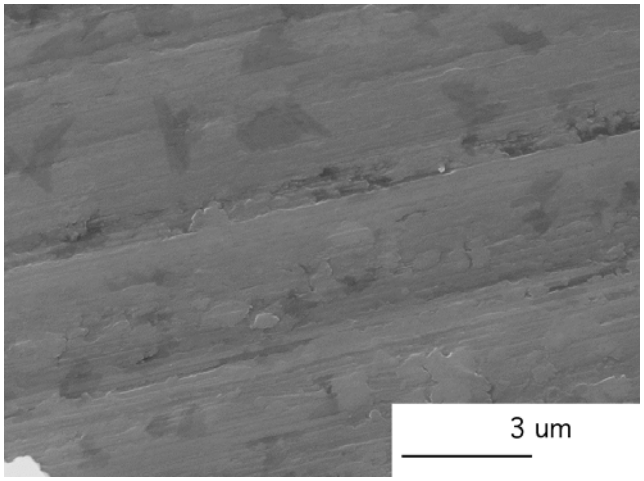

Figure 4.7: During initial beam fabrication, the induced surface flaws caused catastrophic failure before load plateaus.

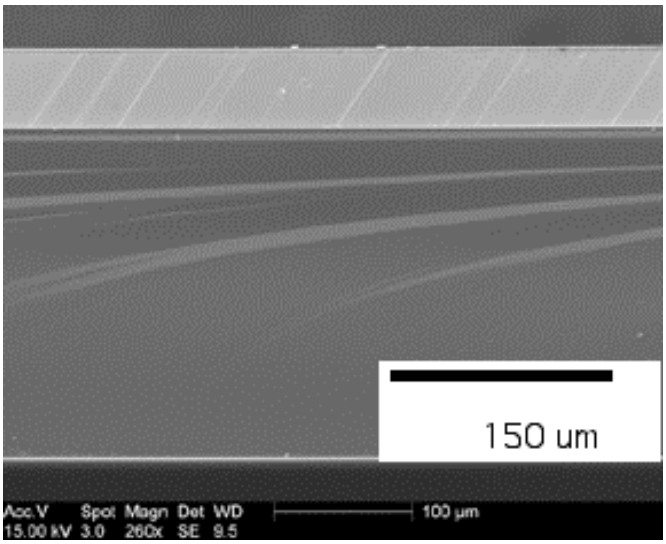

Figure 4.8: Cross section of the Si beam after etching.

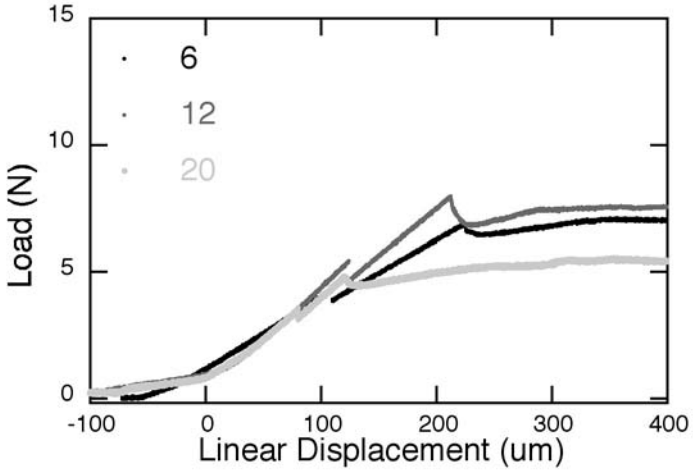

Figure 4.9: The load-displacement curves for 6nm, 12nm and 20nm Ti interlayers are shown.

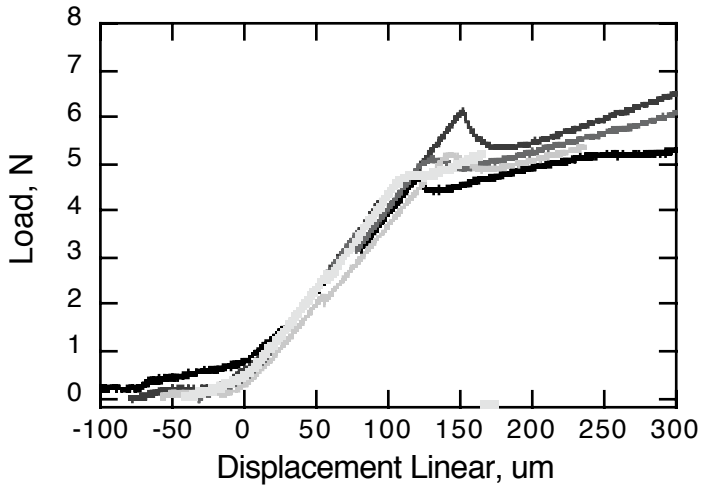

Figure 4.10: The load-displacement curves for five samples having a 12 nm thick Ti interlayer are shown. The initial plateau was averaged over 20 μm.

4.4 Stressed Overlayer Four Point Bend Comparison

The practical fracture energies are shown in Figure 4.14 and the mode I fracture energies for these two techniques are shown in Figure 4.15. Both measurement techniques showed an increase in adhesion energy until a film thickness of 12nm was reached and then a reduction in fracture energy as the thickness increased to 20nm. Due to the differences in phase angle of loading, one would expect a higher practical toughness for the buckles than the four point bending tests, as is observed in Figure 4.14. The differences between the two test methods are most likely due to the differences in phase angles of testing. (these are the inferred mode one toughness values calculated using eq. 2.18). The factor of two to three difference between the mode I values are due to the high phase angle of testing for the buckles. As eq. 2.18 demonstrates, the practical work of adhesion increases dramatically as the phase angle approaches 90º. Therefore, small errors in the technique will be amplified when a mode I value is extracted. Similarly, the assumptions used in the empirical experimental analysis of eq. 2.18 are not certain. When eq. 2.18 was developed, it was for one set of brittle materials, and we have extended it's use to materials which do exhibit plastic deformation. Therefore, while the difference between mode I toughness values is relatively large, the similarity in trends suggests both methods are viable methods for evaluating toughness within material systems with similar properties (i.e. plastically deforming metals on dielectric substrates).

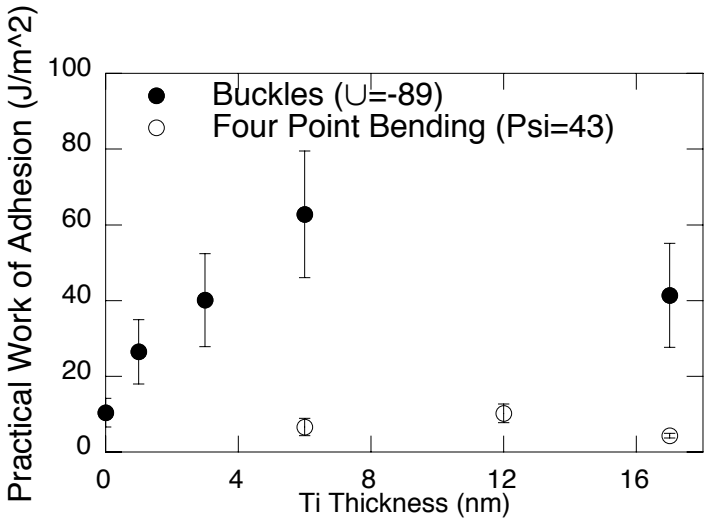

Figure 4.11: Mixed mode fracture energies taken by buckle and four-point bend methods as a function of nominal Ti interlayer thickness are shown.

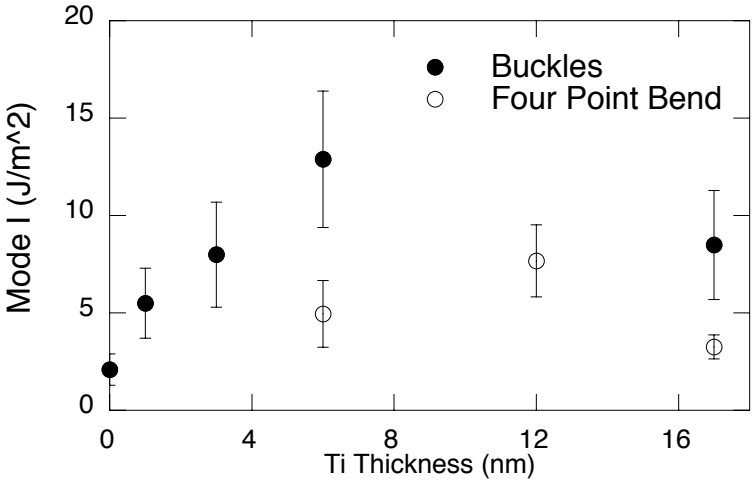

Figure 4.12: Mode I fracture energies as a function of nominal Ti interlayer thickness.

4.5 References

[1] Schneider JA, Guthrie SE, Kriese MD, Clift WM, Moody NR. Impurity effects on the adhesion of aluminum films on sapphire substrates. Materials Science & Engineering A: Structural Materials: Properties, Microstructure and Processing 1999;A259:253.

[2] Kennedy MS, Zosel M, Richards CD, Richards RF, Bahr DF, Hipps KW, Moody NR. Optimization of film stresses utilized in composite piezoelectric membrane microgenerators. vol. 795. Boston, MA., United States: Materials Research Society, 2003. p.503.

[3] Duval FFC, Dorey RA, Haigh RH, Whatmore RW. Stable TiO_2/Pt electrode structure for lead containing ferroelectric thick films on silicon MEMS structures. Thin Solid Films 2003;444:235.
[4] Kennedy MS, Bahr DF, Richards CD, Richards RF. Residual stress control to optimize PZT MEMS performance. vol. 741. Boston, MA, United States: Materials Research Society, 2002. p.163.
[5] Tu KN. Surface and interfacial energies of $CoSi_2$ and Si films. Implications regarding formation of three-dimensional silicon-silicide structures. IBM Journal of Research and Development 1990;34:868.
[6] Burton WK, Cabrera N, Frank FC. The Growth of Crystals and the Equilibrium Structure of their Surfaces. Philosophical Transactions of the Royal Society of London. Series A, Mathematical and Physical Sciences 1951;243:299.
[7] Oberhauser P, Abermann R. Influence of substrate properties on the growth of titanium films: Part III. Thin Solid Films 1999;350:59.
[8] Godfroid T, Gouttebaron R, Dauchot JP, Leclere P, Lazzaroni R, Hecq M. Growth of ultrathin Ti films deposited on SnO_2 by magnetron sputtering. Thin Solid Films 2003;437:57.
[9] Cui Z, Ngo S, Dixit G. A sample preparation method for four point bend adhesion studies. Journal of Materials Research 2004;19:1324.
[10] Gan Z, Mhaisalkar SG, Chen Z, Zhang S, Chen Z, Prasad K. Study of interfacial adhesion energy of multilayered ULSI thin film structures using four-point bending test. Surface and Coatings Technology 2005;198:85.
[11] Zhenjiang C, Dixit G, Li-Qun X, Demos A, Kim BH, Witty D, M'Saad H, Dauskardt RH. Benchmarking four point bend adhesion testing: the effect of test parameters on adhesion energy. AIP Conference Proceedings 2005:507.
[12] Ma Q, Bumgarner J, Fujimoto H, Lane M, Dauskardt RH. Adhesion measurement of interfaces in multilayer interconnect structures. Materials Reliability in Microelectronics VII. Symposium 1997:3.

5.0 Conclusions

Adhesion and fracture of thin films and interfaces affects the performance and reliability of macro and micro devices. For design of new MEMs and microelectronic devices, there is a need for uniform measurement of adhesion and increased understanding of contribution factors to adhesion. There are several techniques for quantitatively measuring the adhesion energies of film systems, including indentation induced, residual stress driven, scratch induced and four point bending. All of these methods can only be used for some film systems, depending on a range of factors including the initial strength of the interface. Initial comparisons suggested that plasticity of the film and substrate and also fracture within these components led to both underestimations and overestimations in the calculated fracture energies since current models do not account for plasticity and fracture within the film.

For systems where fracture only occurs along the interface, such as Au/Si, the calculated fracture energies are identical if the energy put into the system is kept near the needed strain energy release rate to cause delamination. Overlayers of different stresses and thickness on Au/Si showed that the calculated adhesion energies could change by a factor of four when high stresses lead to much higher strain energies than needed for delamination. The Pt film system was used to compare four point bending and spontaneous buckles showed similar trends but not identical adhesion values. The reason for the variation of Mode I values was the use of an empirical formula that causes in accuracies in extrapolating from mixed mode to mode I values.

The benefit of the four point bend test is that the phase angle is well controlled and therefore likely provides a more accurate value of toughness. However, several wafers of materials must be fabricated and extreme care is required to perform these tests. Also, the toughness of the interface, if too great, may not allow fracture at the appropriate interface, and instead the epoxy bonds used in the sample fabrication may mail. With limited sample material conditions (for instance in many MEMS or with samples from the field) the overlayer tests provide a reasonable measurement of toughness. Most importantly, the trends in measuring toughness appear to track between the two methods, suggesting if two material conditions are to be evaluated (i.e. exposure to different hydrogen exposures), the test method most appropriate for the sample geometry can be used with confidence to predict trends in changes in adhesion in thin film systems.

Distribution:

3 Professor David Bahr
Washington State University
School of Mechanical and Materials Engineering
PO Box 642920
Pullman, WA 99164-2920

3 Professor Marian S. Kennedy
Clemson University
113 Olin Hall
Clemson, SC 29634

1	MS 0346	E. D. Reedy, Jr., 1526
1	MS 1245	J. A. Emerson, 2453
1	MS9161	A. E. Pontau, 8750
1	MS9402	R. A. Causey, 8758
3	MS 9402	N. R. Moody, 8758
1	MS 9402	X. Zhou, 8776
1	MS 9404	E-P Chen, 8776
1	MS 9042	J. W. Foulk, 8776
1	MS 9409	J. A. Zimmerman 8776
1	MS 0123	D. Chavez, LDRD Office, 1011
2	MS 0899	Technical Library, 9535
2	MS 9018	Central Technical Files, 8944